RSC Advances

RSC Publishing

PAPER

View Article Online
View Journal | View Issue

Cite this: *RSC Advances*, 2013, **3**, 14509

A novel fluoro-terminated hyperbranched poly(phenylene oxide) (FHPPO): synthesis, characterization, and application in low-*k* epoxy materials

Lijuan Luo,[ab] Teng Qiu,[a] Yan Meng,*[b] Longhai Guo,[a] Jing Yang,[c] Zhuoxin Li,[c] Xingzhong Cao[c] and Xiaoyu Li*[a]

Received 10th February 2013,
Accepted 13th May 2013

DOI: 10.1039/c3ra40721g

www.rsc.org/advances

A new AB_2 monomer 4-hydroxyl-4′,4′′-difluorotriphenylmethane was successfully synthesized *via* a Friedel–Crafts alkylation of phenol from 4,4′-difluorodiphenylmethanol. Based on the AB_2 monomer, novel fluoro-terminated hyperbranched poly(phenylene oxide)s (FHPPOs) were synthesized *via* the S_NAr reaction by self-condensation in one step. The FHPPOs were characterized by various techniques, including NMR, FT-IR, GPC, TGA and DSC. It was found that the molecular weight and polydispersity index of the FHPPOs increased with monomer concentration and reaction time. The degree of branching of the FHPPOs, determined by ^{13}C NMR and ^{19}F NMR with the aid of model compounds, decreased from 0.63 to 0.53 as the molecular weight increased. The glass transition temperature (T_g) of the FHPPOs increased with increasing molecular weight, up to 164 °C when the M_n was over 6, 800. The FHPPOs showed excellent thermal stability up to a T_{d5} temperature of 559 °C. Because of the low polarity of the poly(phenyl oxide) (PPO) backbones, abundant fluoro-terminated groups, which have large molar free volume, low polarizability of C–F bonds, and inherent free volume or molecule-scale cavities in hyperbranched structures, the addition of FHPPO into diglycidyl ether of bisphenol A (DGEBA) could effectively lower the relative dielectric constant, the dissipation factor, and moisture absorption of the cured DGEBA/FHPPO composites. The free volume of the composites, which was quantified by positron annihilation lifetime spectroscopy (PALS), increased with increased FHPPO loading. The excellent dielectric and thermal properties make FHPPO a promising low-*k* modifier for epoxy resins.

Introduction

Since the pioneering work of Kim and Webster, hyperbranched polymers have attracted lots of attention and are now at the forefront of polymer research.[1–5] Unlike linear polymers, hyperbranched polymers (HBPs) are highly branched three-dimensional macromolecules and have inherent internal cavities and abundant terminal groups, which often lead to better processability, compatibility and solubility.[6] Hyperbranched polymers have been used as rheology modifiers, processing aids, and more recently, as functional materials in coatings, catalysts, sensors, bio-materials, emitting materials, and in nano-templating applications.[6–12]

Unlike dendrimers, hyperbranched polymers can be synthesized through one-pot or pseudo-one step procedures but still share most of the properties of dendrimers, which makes them easier and cheaper for commercialization.[4] Recently, several hyperbranched poly(arylene ether)s have been reported, including poly(ether sulfone),[13–16] poly(ether ketone),[17–21] and poly(arylene ether phosphine oxide)s).[22–26] The monomers used to prepare these hyperbranched polymers contain electron-withdrawing groups, *i.e.*,

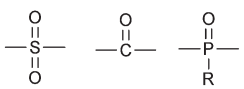

in *ortho* and *para* positions of the leaving groups, which can serve as the activating groups and are favourable for aromatic nucleophilic substitution (S_NAr) reactions. However, only a handful of research has reported on the synthesis of hyperbranched poly(phenyl oxide) (HPPO) *via* S_NAr reactions because the monomers used for preparing HPPO lack the

[a]*State Key Laboratory of Organic and Inorganic Composites, Beijing University of Chemical Technology, Beijing 100029, P. R. China. E-mail: lixy@mail.buct.edu.cn; Tel: +8610-64419631*
[b]*Key Laboratory of Carbon Fiber and Functional Polymers, Ministry of Education, Beijing University of Chemical Technology, Beijing 100029, P. R. China. E-mail: mengyan@mail.buct.edu.cn; Fax: +8610-64452129; Tel: +8610-64419631*
[c]*Key Laboratory of Nuclear Analysis Techniques, Institute of High Energy Physics, Chinese Academy of Science, Beijing 100049, P. R. China*

necessary activating groups as mentioned above, which greatly limit the applications of HPPOs.

As an important engineering plastic, poly(phenyl oxide) (PPO) has outstanding thermal, mechanical and dielectric properties.[27,28] However, its poor moldability, poor solubility and inadequate adhesive strength limits its applications. Compared with linear polymers, hyperbranched polymers have lower viscosity and better solubility due to their abundant functional groups and semi-global shape.[4] As a result, hyperbranched poly(phenyl oxide) (HPPO) could combine the benefits of PPO with the merits of hyperbranched polymers. Therefore, it is important to design new HPPOs with specific structures and terminal groups to expand their applications. Kim *et al.*[18] reported a bromo-terminated HPPO, which was derived from 3,5-dibromophenol by the Ullmann reaction. However, applications of this HPPO have not been reported until now, which is probably because of the poor ability of the chemical modifications and the low functionality of the terminal aryl bromide groups in the HPPO. A series of hyperbranched poly(arylene ether)s based on 3,5-bis-(4-fluoro-3-trifluoro-methylphenyl) phenol using the AB + AB_2 and A_2 + AB_2 approaches have been reported by Ghosh and coworkers.[29,30] Using the A_2 + B_3 approach, Banerjee[31] also reported a hyperbranched poly(arylene ether), which shared similar chemical structure with those of Ghosh's. They successfully introduced the trifluoromethyl groups in the *ortho* positions of the leaving groups, which notably improved the reactivity of the monomers. Those hyperbranched polymers with abundant fluorinated substituents had high glass transition temperatures (T_gs), good thermal stabilitiy and hydrophobicity. However, further applications for those hyperbranched polymers have not yet been reported, probably due to the poor processability and the high cost of the raw materials.

In our previous studies,[32,33] HPPO was prepared from 4-bromo-4′,4′′-dihydroxyltriphenylmethane by the Ullmann reaction using CuCl as the catalyst. The phenolic terminated HPPOs can be easily modified and used in epoxy resins,[34] bismaleimide resins,[35] and cyanate ester resins.[36] In another work of ours,[37] the Ullmann reaction was replaced by the S_NAr reaction, and HPPO was synthesized using 4-fluoro-4′,4′′-dihydroxyl triphenyl methane as an AB_2 monomer. Subsequently, the synthesized HPPO was used as a modifier for epoxy resins and both the mechanical and thermal properties of the modified epoxy systems were improved. In those cases, the terminal groups of HPPO were phenolic groups. It is believed that the terminal groups of hyperbranched polymers can greatly affect the macromolecular properties, *e.g.*, the glass transition temperature (T_g), the solubility, dielectric properties, hydrophobicity, and thermal stability. Thus, in this work, the terminal groups of the HPPO macromolecule are changed into fluorinated substituents and those FHPPOs are synthesized using 4-hydroxyl-4′,4′′-difluorotriphenylmethane as an AB_2 monomer through the S_NAr reaction. The effects of monomer concentration and reaction time on the molecular weight, degree of branching (DB), glass transition temperature (T_g), and thermal stability of HPPO were investigated. By virtue of the low polarity of the basic units of PPO, abundant fluorinated terminal groups, and the inherent free volume (or cavities) in the hyperbranched structures, the reported hyperbranched macromolecules could have potential applications in low-*k* materials.

Experimental

Materials

Phenol (98%) was purchased from Tianjin Chemical Reagents Factory, China. 4,4′-difluorodiphenylmethanol (99%) was purchased from Changzhou Rising Chemical Co. Ltd., China. Fluorobenzene (99%) and 2-ethyl-4-methylimidazole (2E4MZ, 99%) were obtained from Acros Organics. Other solvents were purchased from Beijing Chemical Works, China. Diglycidyl ether of bisphenol A (DGEBA) was purchased from Yueyang Resin Factory, China (epoxy equivalent weight, EEW = 186.2 g/equiv.). Methyl nadic anhydride (MNA) (99.8%) was supplied by POLYNT Chemical Co. Ltd., Italy. All the reagents and solvents were used as received without further purification.

Synthesis of AB_2 monomer: 4-hydroxyl-4′,4′′-difluorotriphenylmethane (compound 2)

A solution of phenol (42.0 g, 0.447 mol) and H_2SO_4 (20 ml) in CH_2Cl_2 (250 ml) was cooled to 5 °C, then a solution of 4,4′-difluorodiphenylmethanol (87.6 g, 0.4 mol) in CH_2Cl_2 (250 ml) was added dropwise with mechanical stirring. After maintaining at 5 °C for 6 h, the organic phase of the mixture was treated with a saturated aq. $NaHCO_3$ solution and extracted with ethylacetate. The organic layer was dried with anhydrous $MgSO_4$ and concentrated under vacuum, and the obtained crude product was recrystallized by 2 : 1 hexane/toluene. Finally, the obtained compound 2 was dried under vacuum at 80 °C thoroughly to give a yellow semi-solid (65.1 g, 55%).

In order to determine all the products, 2 g crude product was purified by silica gel column chromatography using 1 : 1 CH_2Cl_2/petroleum ether as the eluent. After drying under vacuum at 80 °C, desired AB_2 momoner (denoted as **2** in Schemes 1 to 3) (1.1 g, 60%) and by-product (denoted as **2′** in Scheme 2) (0.7 g, 39%) were obtained.

Compound 2. Purity (UPLC): 96.5%; MS *m*/*z* 295.3 (M^-); ^{1}H NMR, δ_H (600 MHz; $CDCl_3$; Me_4Si) 4.67 (1H, s, O**H**), 5.44 (1H, s, C**H**), 6.77 (2H, d, $C_6\mathbf{H}_4OH$), 6.93 (2H, d, $C_6\mathbf{H}_4OH$), 6.97 (4H, t, $C_6\mathbf{H}_4F$), 7.02 (4H, m, $C_6\mathbf{H}_4F$); ^{13}C NMR, δ_C (600 MHz; acetone-d6; Me_4Si) 54.41, 115.07, 115.25, 130.37, 130.66, 135.91, 139.71, 154.08, 160.61.

Compound 2′. Purity (UPLC): 96.4%; MS *m*/*z* 497.7 (M^-); ^{1}H NMR, δ_H (600 MHz; $CDCl_3$; Me_4Si) 5.33 (1H, s, O**H**), 5.67 (2H, s, C**H**), 6.40 (1H, d, $C_6\mathbf{H}_3O$), 6.76 (1H, d, $C_6\mathbf{H}_3O$), 6.83 (1H, q, $C_6\mathbf{H}_3O$), 6.93 (2H, d, $C_6\mathbf{H}_3OH$), 6.93 (8H, m, $C_6\mathbf{H}_4F$), 6.96 (8H, m, $C_6\mathbf{H}_4F$); ^{13}C NMR, δ_C (600 MHz; acetone-d6; Me_4Si) 49.02, 54.34, 115.12, 115.87, 128.60, 130.47, 130.52, 131.37, 136.00, 138.01, 139.62, 151.69, 162.20.

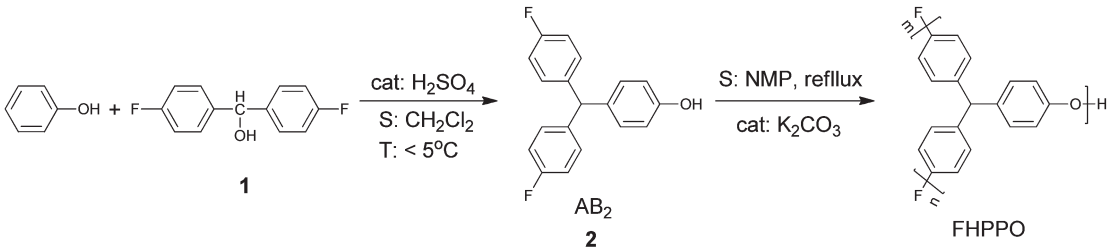

Scheme 1 Synthesis route of fluoro-terminated hyperbranched poly(phenylene oxide) (FHPPO).

Synthesis of fluoro-terminated hyperbranched poly (phenylene oxide) (FHPPO)

AB_2 (35.5 g, 0.12 mol) monomer (compound 2) and potassium carbonate (21.5 g, 0.156 mol) were added into a mixture of *N*-methylpyrrolidone (NMP) (600 ml) and toluene (150 ml). After refluxing for 3 h, the water produced in the reaction was removed by a Dean–Stark trap. Subsequently, the temperature was elevated to 202 °C. After 2 days, the mixture was cooled to room temperature and poured into 1500 ml of 10% acetic acid solution. The precipitate was collected and reprecipitated from THF into methanol. The resultant off-white solids were dried under a vacuum at 60 °C (28.4 g, 80%). ^{1}H NMR, δ_H (600 MHz; $CDCl_3$; Me_4Si) 5.44 (s, C**H**(C_6H_5)$_3$), 6.89 (br s, C_6**H**$_4$), 7.01 (br s, C_6**H**$_4$); ^{13}C NMR, δ_C (600 MHz; $CDCl_3$; Me_4Si) 54.57, 115.11, 115.31, 130.48, 130.67, 138.37, 155.66, 160.67.

Synthesis of model compound 3 (MC3)

AB_2 monomer (4.72 g, 16 mmol), fluorobenzene (16.00 g, 160 mmol), and potassium carbonate (4.42 g, 32 mmol) were added into 140 ml of NMP. The mixture was refluxed under nitrogen and stirred for 72 h. It was then cooled to room temperature, filtered, and slowly precipitated in 10 wt% acetic acid solution. The crude precipitate was purified by silica gel column chromatography using 1 : 2 CH_2Cl_2/petroleum ether as the eluent. After drying under a vacuum at 80 °C, a white solid was obtained (2.5 g, 42%). Purity (UPLC): 96.6%; ^{1}H NMR, δ_H (600 MHz; $CDCl_3$; Me_4Si) 5.52 (1H, s, C**H**), 6.97 (2H,

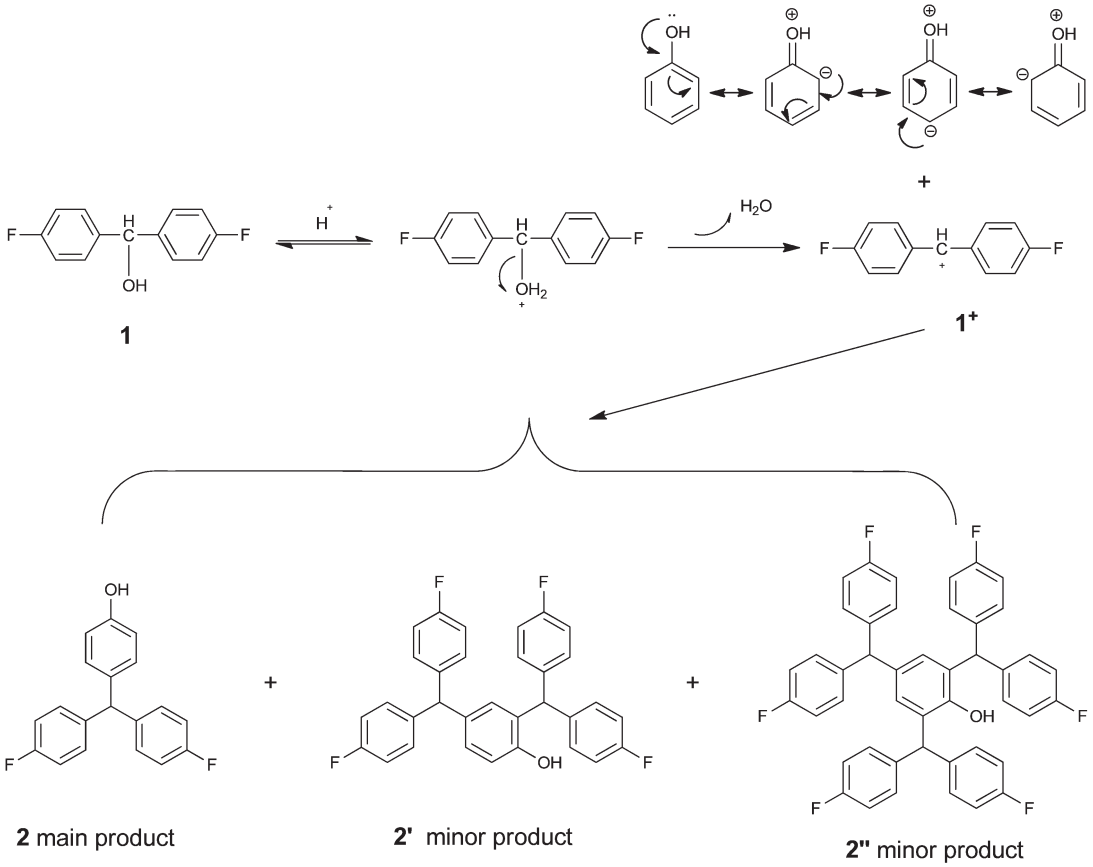

Scheme 2 Synthetic mechanisms of AB_2 monomer.

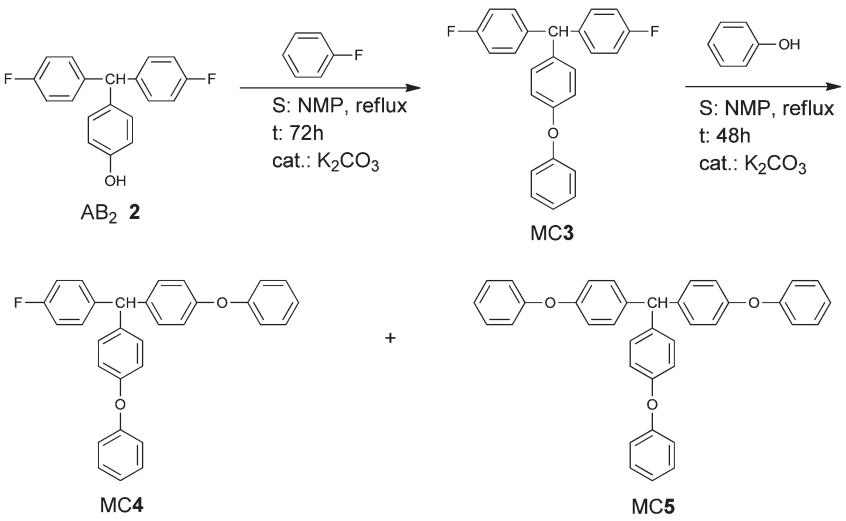

Scheme 3 Synthesis route of model compounds.

d, $C_6\mathbf{H}_5O$), 7.01 (4H, m, $C_6\mathbf{H}_4F$), 7.04 (2H, d, $C_6\mathbf{H}_4O$), 7.06 (2H, d, $C_6\mathbf{H}_4O$), 7.09 (4H, m, $C_6\mathbf{H}_4F$), 7.12 (1H, t, $C_6\mathbf{H}_5O$), 7.35(2H, t, $C_6\mathbf{H}_5O$); ^{13}C NMR δ_C (600 MHz; acetone-d6; Me_4Si) 54.6, 115.3, 118.7, 119.0, 123.4, 129.8, 130.5, 130.8, 138.3, 139.6, 155.9, 157.1, 160.7.

Synthesis of model compounds 4 (MC4) and 5 (MC5)

MC**3** (1.70 g, 4.57 mmol), phenol (0.64 g, 6.86 mmol), and potassium carbonate (1.23 g, 8.91 mmol) were added into a mixture of NMP (40 ml) and toluene (30 ml). The mixture was refluxed for 3 h with water collected in a Dean–Stark trap. Subsequently, the temperature of the mixture was kept at 202 °C for 24 h. At the end of the reaction, the mixture was cooled to room temperature and poured into 10 wt% acetic acid solution. The crude precipitate was purified by silica gel column chromatography using 1 : 2 CH_2Cl_2/petroleum ether as the eluent. The resultant product was dried under a vacuum at 80 °C. Finally MC**4** (0.9 g, 88%) and MC**5** (0.82 g, 69%) were obtained.

MC4. Purity (UPLC): 97.4%; ^{1}H NMR, δ_H (600 MHz; $CDCl_3$; Me_4Si) 5.50 (1H, s, C**H**), 6.95 (4H, d, $C_6\mathbf{H}_5O$), 7.00 (2H, t, $C_6\mathbf{H}_4F$), 7.04 (4H, d, $C_6\mathbf{H}_4O$), 7.06 (4H, d, $C_6\mathbf{H}_4O$), 7.12 (2H, d, $C_6\mathbf{H}_4F$), 7.10 (2H, t, $C_6\mathbf{H}_5O$), 7.34 (4H, t, $C_6\mathbf{H}_5O$); ^{13}C NMR, δ_C (600 MHz; acetone-d6; Me_4Si) 54.7, 115.1, 118.6, 118.9, 123.3, 129.7, 130.5, 130.7, 138.6, 140.0, 155.8, 157.1, 160.6.

MC5. Purity (UPLC): 98.2%; ^{1}H NMR, δ_H (600 MHz; $CDCl_3$; Me_4Si) 5.50 (1H, s, C**H**), 6.95 (6H, d, $C_6\mathbf{H}_5O$), 7.03 (6H, d, $C_6\mathbf{H}_4O$), 7.08 (6H, d, $C_6\mathbf{H}_4O$), 7.10 (3H, br s, $C_6\mathbf{H}_5O$), 7.33 (6H, t, $C_6\mathbf{H}_5O$); ^{13}C NMR, δ_C (600 MHz, acetone-d6, Me_4Si): 54.8, 118.6, 118.9, 123.2, 129.7, 130.5, 138.8, 155.7, 157.2.

Preparation of DGEBA/FHPPO composites

Different amounts of FHPPO_2, *i.e.*, 3, 5, 10, 15, and 20 wt% of the total weights, were added into the stoichiometric mixtures of DGEBA and MNA. The accelerator, 2E4MZ (1 wt% of weight of the DGEBA) was then added under continuous stirring at 60 °C. In order to obtain a homogeneous mixture, a small amount of tetrahydrofuran (THF) was used. The homogeneous mixtures were degassed in a vacuum oven at 80 °C and then cured in silicone rubber molds. The curing schemes are as follows: 120 °C for 2 h, 160 °C for 2 h, and 200 °C for 2 h.

Characterizations

The ^{1}H and ^{13}C NMR spectra were collected using a Bruker Fourier Transform AVANCE 600 spectrometer. The ^{19}F NMR spectra were collected using a Bruker Fourier Transform AVANCE 400 spectrometer. $CDCl_3$ were used in all NMR measurements as solvents. Acquisition parameters were optimized for quantitative ^{13}C NMR measurements, including a 4.2-microsecond 45° pulse, inverse gated proton decoupling and a 5 s delay time between pulses. A total of 2500 scans were used for data averaging. For quantitative ^{19}F NMR, a 7.5-microsecond 45° pulse, inverse gated proton decoupling, an 8 s delay time between pulses, and a total of 64 scans were used.

Gel permeation chromatography (GPC) diagrams were obtained with a Waters GPC 515-2410 system equipped with 2410 refractive index detector and Styragel column (HT3_HT5_HT6E) using tetrahydrofuran as the eluent at 30 °C. The GPC columns were calibrated with linear narrow polystyrene standards of known molecular weights in the range of 160 to 85 000 000. The molecular weights (in g mol^{-1}) of the samples are rounded to the nearest hundred.

The infrared spectra of samples in the form of KBr pellets were recorded on a Bruker Tensor 37 spectrometer at room temperature. Mass spectra were obtained from a Waters Quattro Premier XE with methanol as the solvents.

Purity of all synthesized compounds was determined by a Waters Acquity Ultra Performance LC equipped with a TUV detector. The analytical column was a Waters BEH C18, 50 × 2.1 mm (1.7 μm). The mobile phase consisted of methanol and ultra-pure water. A linear gradient was used to ramp the mobile phase composition from 30% (v/v) water to 1% (v/v) water in 6 min. The runtime was 8 min per sample. The flow rate was 0.25 mL min^{-1} and the column oven temperature was set at 40 °C. UV absorption was monitored at 235 nm.

The glass transition temperatures were determined by a METTLER DSC1 differential scanning calorimetry on second heating runs at a heating rate of 10 K min^{-1} under nitrogen. Thermal stability was measured using a Perkin-Elmer Pyris1 thermogravimetric analyzer (TGA) from 50 to 750 °C at a heating rate of 20 K min^{-1} under nitrogen.

Values of the dielectric constant and dissipation factor of cured samples were characterized by an Anton Paar MCR 301 rheometer with a dielectro-rheological device (DRD) at 30 °C. The test samples were round disks with a diameter of 25.0 mm and a thickness of 2.0 mm.

Moisture absorption measurements were tested using the following procedure: samples in the size of 60.0 mm × 12.8 mm × 3.2 mm were dried under vacuum at 100 °C to remove all moisture. After cooling to room temperature, the specimens were weighed. Then they were placed in boiling water for 2 h and weighed again. The moisture absorption (MA) was calculated as

$$MA = (w/w_0 - 1) \times 100\% \quad (1)$$

where w is the sample weight after boiling water treatment, and w_0 is the sample weight before placing in water.

Positron annihilation lifetime spectroscopy (PALS) was used to determine the free volumes or cavities of the cured DGEBA/FHPPO composites. Detailed background information on the theory and techniques of PALS can be found elsewhere.[38,39] Generally speaking, the lifetimes and intensities of positrons, which are generated from a ^{22}Na source, are measured and used to estimate the local free volumes inside polymers. Once inside the polymers, the positron forms one of the two possible types of positroniums, *i.e.*, an *ortho*-positronium or a *para*-positronium, which can pair with electrons abstracted from the environment. After proper curve fitting, the lifetimes of the various species and their intensity can be determined from the decay spectra of positrons. In particular, the lifetime of *ortho*-positronium (τ_3) and intensity (I_3) are found to be correlate well with the local free volume in polymers,[40–42] in which τ_3 corresponds to the size of individual free volume sites and I_3 corresponds to their number concentration.

Results and discussions

Synthesis of AB_2 monomer

In the AB_2 monomer, the phenolic group and fluorine group are represented by A and B, respectively. The synthesis route of the AB_2 monomer is shown in Scheme 1. The monomer can be synthesized easily and cheaply with the commercially available 4,4′-difluorodiphenylmethanol and phenol. The AB_2 monomer, 4-hydroxyl-4′,4′′-difluorotriphenylmethane, was synthesized successfully by Friedel–Crafts alkylation using H_2SO_4 as the catalyst in CH_2Cl_2 solvent. The structure of compound AB_2 was characterized by ^1H NMR, ^{13}C NMR, and MS. The byproduct compound **2′**, which was obtained by column chromatography separation, was also determined by ^1H NMR, ^{13}C NMR and MS. The spectra of ^{13}C NMR and the assignments of each peak of AB_2 monomer (**2**) and compound **2′** are shown in Fig. 1.

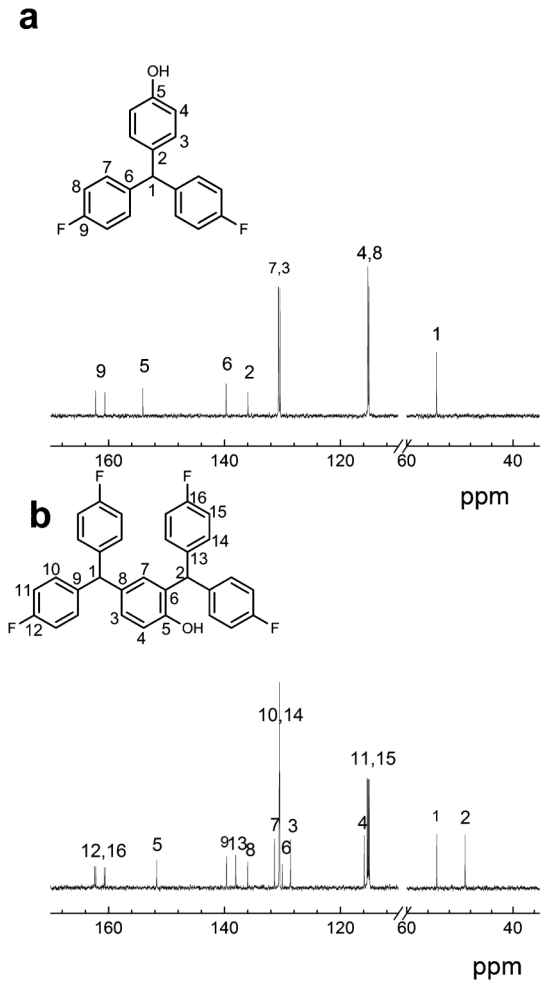

Fig. 1 ^{13}C NMR spectra of compounds of 2 (a) and 2′ (b).

The mechanism of the Friedel–Crafts alkylation is shown in Scheme 2. Firstly, compound **1** (4,4′-difluorodiphenylmethanol) produces a stable carbocation $\mathbf{1}^+$ under the protonation of H_2SO_4. Then, a proton transfers from the oxygen to the carbon atom, and the *para* and *ortho* positions are electron-rich. Carbocation $\mathbf{1}^+$ is captured by the *para* position of phenol to form the main product **2**; carbocations $\mathbf{1}^+$ are captured by the *para*- and *ortho*-positions of phenol to form the byproducts **2′** and **2′′**. Considering the steric hindrance of $\mathbf{1}^+$ in the *ortho*-substitution, compound **2** is the main product, and no compound **2′′** is found in this reaction. In order to further increase the yield of compound **2**, low temperature (<5 °C) and excess phenol could be used.

Synthesis of fluoro-terminated hyperbranched poly(phenyl oxide)

Using the nucleophilic aromatic substitution (S_NAr) reaction, a series of fluoro-terminated hyperbranched poly(phenylene oxide) with different molecular weights, (FHPPO)s, were prepared by one-step polymerization of 4-hydroxyl-4′,4′′-difluorotriphenylmethane

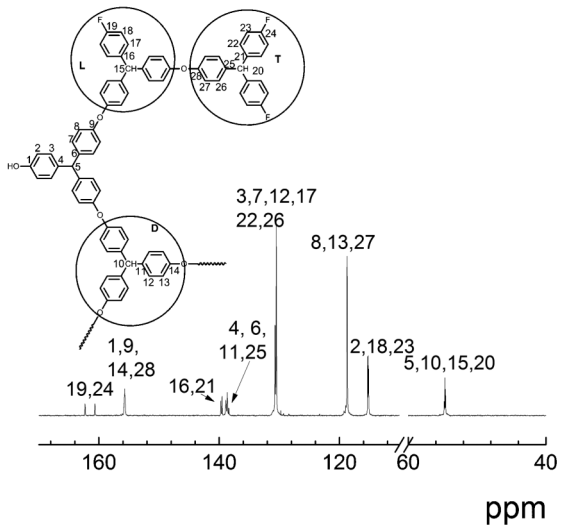

Fig. 2 The ^{13}C NMR spectrum of FHPPO.

(AB_2 monomer '**2**'), as shown in Scheme 1. The chemical structure of the FHPPO was determined by ^{13}C NMR and FT-IR measurements, as shown in Fig. 2 and 3, respectively. The assignments of peaks of ^{13}C NMR are shown in Fig. 2. In the FT-IR spectrum, the peaks at 1599 and 1498 cm^{-1} correspond to the stretching vibrations of aromatic rings; the peaks at 1236 and 825 cm^{-1} correspond to the Ph–O–Ph stretching and the Ph–H distorting, respectively; the broad band at about 3400 cm^{-1} corresponds to stretching vibration of phenolic hydroxyl groups.

In our previous studies,[32,33] HPPOs were prepared from 4-bromo-4′, 4′′-dihydroxyltriphenylmethane by the Ullmann reaction using CuCl as the catalyst. However, it was difficult to remove all the copper salt in the reaction system. Thus, the S_NAr reaction is used to replace the Ullmann reaction in this study. In order to take advantages of the desirable properties of the fluorinated substituents, such as low polarizability of C–F bonds,[43] low moisture absorption, and good solubility, HPPO with abundant fluoro-terminated groups was synthesized by the S_NAr reaction using 4-hydroxyl-4′,4′′-difluorotriphenylmethane as the AB_2 monomer.

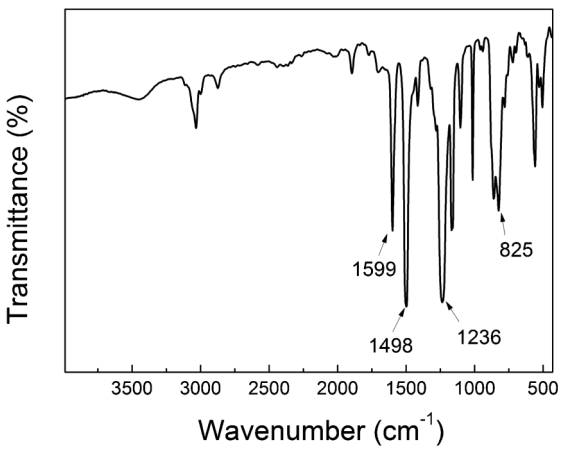

Fig. 3 The FT-IR spectrum of FHPPO.

In the S_NAr reaction, linkages are formed by the reaction between a phenolic group and a leaving group in the presence of a suitable base, such as potassium carbonate. Because 4-hydroxyl-4′,4′′-difluorotriphenylmethane does not have any activating groups in the *ortho* or *para* positions of the leaving group, polar solvents with high boiling points, *N*-methylpyrrolidone (NMP), along with K_2CO_3, were used in order to produce the phenolate ion. In order to increase the average molecular weight, a mixture of NMP and toluene was used to remove the water produced at the very beginning of the reaction.

In general, high monomer concentration and long reaction time are beneficial for increasing the molecular weight. As shown in Table 1, the average molecular weight number (M_n) and the polydispersity index (PDI) of FHPPO increase with reaction time and monomer concentration. In order to check the reproducibility, FHPPO_2 was repeated three times under the same reaction conditions. The M_ns and PDIs from different experiments are very close: for the first batch, $M_n \sim 2500$, PDI $\sim$ 2.2; for the second batch, $M_n \sim 2800$, PDI $\sim$ 2.2; for third batch, $M_n \sim 2500$, PDI $\sim$ 2.1. The solubilities of the resulting FHPPO_2 and FHPPO_5 in different solvents are summarized in Table 2. Both FHPPOs dissolve well in a variety of common organic solvents, *i.e.*, tetrahydrofuran (THF), dichloromethane (CH_2Cl_2), chloroform ($CHCl_3$), toluene, *N*, *N*-dimethyl formamide (NMF), and *N*-methyl-2-pyrrolidinone (NMP), but not in acetone or methanol. Ethanol, DMSO and ethyl acetate are poor solvents for FHPPO_2, which has a lower molecular weight, but the good solvents for FHPPO_5, which has a higher molecular weight. One explanation may be that the FHPPO with higher molecular weight has much more terminal groups and thus is more soluble than that with lower molecular weights. We note that the solubility of the FHPPO is different from the HPPO synthesized in our previous studies,[32,33] indicating that the terminal groups play a big role in the solubility of hyperbranched polymers.

Degree of branching of FHPPO

Aside from molecular weights and PDI, the degree of branching (DB) is another important parameter for describing hyperbranched molecules. Unlike dendritic molecules, which are essentially perfectly branched and have a DB of 100%, the DB of hyperbranched molecules is less than 100%. The DB can be calculated using NMR spectroscopy. Hawker and Fréchet defined DB as[44]

$$\mathrm{DB} = \frac{D+T}{D+L+T} \quad (2)$$

where D is the number of dendritic units, T is the number of terminal units, and L is the number of linear units.

Since the number of dendritic units is theoretically equal to the number of terminal units plus one, Holter and Frey[45] proposed that for higher molecular weights molecules, eqn (2) is simplified to

$$\mathrm{DB} = \frac{2T}{2T+L} \quad (3)$$

Table 1 Properties of the fluoro-terminated hyperbranched poly(phenylene oxide)s (FHPPOs)

Entry	Time (d)	Concentration (M)	M_n (g mol^{-1})	PDI	T_g (°C)	Yield (%)	T_{d5}[a] (°C)	T_{max}[b] (°C)	Residue at 700 °C, in N_2 (%)	DB[c]	DB[d]	DB[e]
FHPPO_1	2	0.1	20 × 10^2	1.7	135	78	556	601	74.5	0.63	0.64	0.62
FHPPO_2	2	0.2	25 × 10^2	2.2	147	80	559	610	73.9	0.60	0.63	0.61
FHPPO_3	2	0.4	54 × 10^2	3.2	156	86	554	603	72.9	0.56	0.57	0.58
FHPPO_4	4	0.2	58 × 10^2	3.7	163	88	551	604	71.0	0.55	0.57	0.57
FHPPO_5	5	0.2	68 × 10^2	4.8	164	93	549	604	69.8	0.53	0.53	0.56

[a] The temperature at 5 wt% decomposition. [b] The temperature of the maximum decomposition rate. [c] Degree of branching calculated according to Hawker's method using ^{13}C NMR. [d] Degree of branching calculated according to Holter's method using ^{13}C NMR. [e] Degree of branching calculated according to Holter's method using ^{19}F NMR.

where T is the number of terminal units, and L is the number of linear units.

The three types of structural units of FHPPO, *i.e.*, the terminal, linear, and dendritic units, are shown as following:

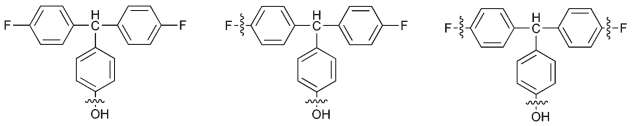

The NMR spectra contain all necessary information for estimating DB. Therefore, model compounds of MC**3**, MC**4**, and MC**5** resembling the terminal, linear, and dendritic structures, respectively, are synthesized to help determine the DBs of the FHPPOs (see Scheme 3). The ^{13}C NMR spectra of MC**3**, MC**4**, MC**5**, and FHPPO (see Fig. 4) are used for the determination of the DBs of the FHPPOs. The chemical shifts at around 54.7 ppm, which correspond to the methylidyne carbons, are the best choice for identifying the numbers of terminal, linear, and dendritic units. Based on the characteristic chemical shifts of methylidyne carbons in MC**3**, MC**4**, and MC**5**, three distinct resonance peaks from lower to higher filed in the spectra of the FHPPO are assigned to the dendritic, linear, and terminal structures, respectively (see Fig. 4). Assuming that the resonance peaks in the FHPPOs are Gaussian and the peak positions are determined from the second derivative of the spectra, the resonance peaks of the FHPPO can be easily deconvoluted to extract the information. For instance, Fig. 4d shows a typical curve-fitting result of the FHPPO. The spectra of each individual component agree well with their corresponding model compounds. Moreover, the reconstructed spectrum, obtained by summing all of the three deconvoluted peaks (shown as a dotted line) match well with the measured spectrum (solid line), indicating the deconvolution process is valid. Following those procedures, the area of each individual peak can be extracted. The DB values of the FHPPO_1–5 based on eqn (2) and based on eqn (3) are calculated and summarized in Table 1.

In addition to ^{13}C NMR, for FHPPO, DB can also be determined from ^{19}F NMR. As shown in Fig. 5, the ^{19}F NMR spectra of MC**3** and MC**4** also show a distinct difference. The two atoms of MC**3** are equivalent and appear as a sharp singlet at −116.4 ppm whereas the single fluorine atom of MC**4** appears at −116.7 ppm. Thus, based on the different resonance peaks of fluorine atoms between terminal and linear structures, DB can also be determined from ^{19}F NMR spectra. Compared with the ^{19}F NMR spectra of model compounds (see Fig. 5), the resonance peaks of FHPPO at a lower field (−116.4 ppm) can be assigned to the terminal units, whereas the resonance at a higher field (−116.7) can be assigned to the linear subunits. Using similar procedures like ^{13}C NMR, the area of each individual peak can be extracted, and the DB values of the FHPPO_1–5 based on eqn (3) were calculated and are summarized in Table 1.

As shown in Table 1, DBs calculated from different methods (^{13}C or ^{19}F; eqn (2) or eqn (3)) all decrease with increasing molecular weight. This trend could be attributed to the difference in reactivity between the two B groups because of the steric hindrance. That is to say, when one B group of the AB_2 monomer reacts with an A group, the other B group in the same AB_2 has less chance to react with the A group. As the molecular weight increases, the hyperbranched molecule becomes bigger, and the terminal B groups on the outside surface become increasingly crowded. The crowding or the steric hindrance effects inhibit the reaction between the second B group and the A group, resulting in a more linear architecture and thus a lower DB. As shown in Table 1, for the same polymer, DBs defined by the Holter's method are slightly higher than those defined by the Hawker's method. Similar results were also reported by another group[24] and could be

Table 2 Solution properties of the fluoro-terminated hyperbranched poly(phenylene oxide)s

Entry	CH_2Cl_2	$CHCl_3$	DMSO	DMF	NMP	Toluene	Ethyl acetate	Acetone	Methanol	Ethanol
FHPPO_2	+	+	±	+	+	+	−	−	−	−
FHPPO_5	+	+	+	+	+	+	+	−	−	−

[a] +, soluble; ±, partially soluble; −, insoluble.

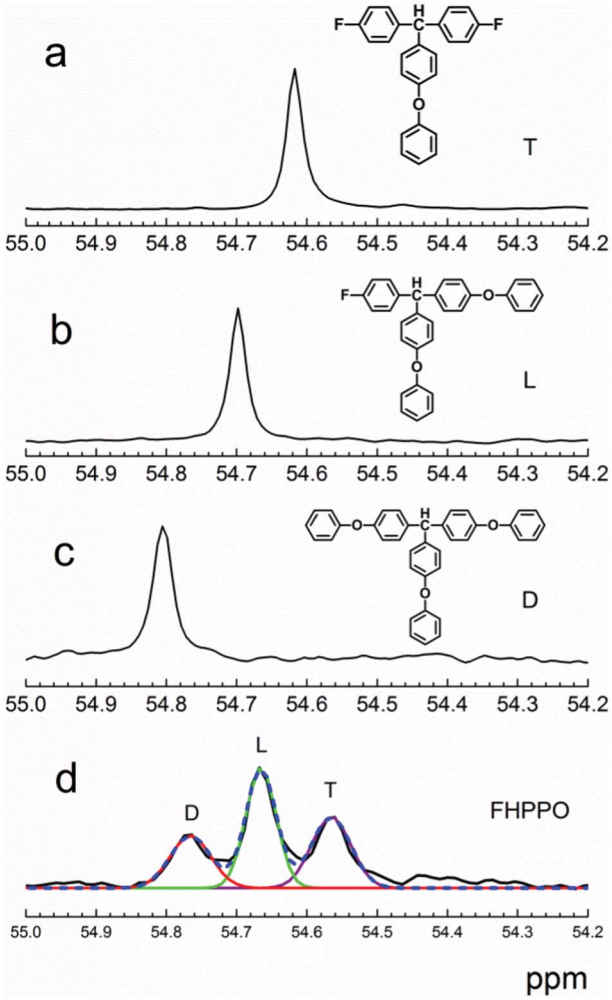

Fig. 4 ^{13}C NMR spectra used to determine the degree of branching of the FHPPO: (a) model compound 3, (b) model compound 4, (c) model compound 5. (d) The deconvoluted resonance peaks of the observed ^{13}C NMR spectra of the FHPPO (solid black line) into the dendritic (D), linear (L), and terminal (T) structures. The reconstructed spectrum (dotted line) was obtained by summing up the three deconvoluted peaks.

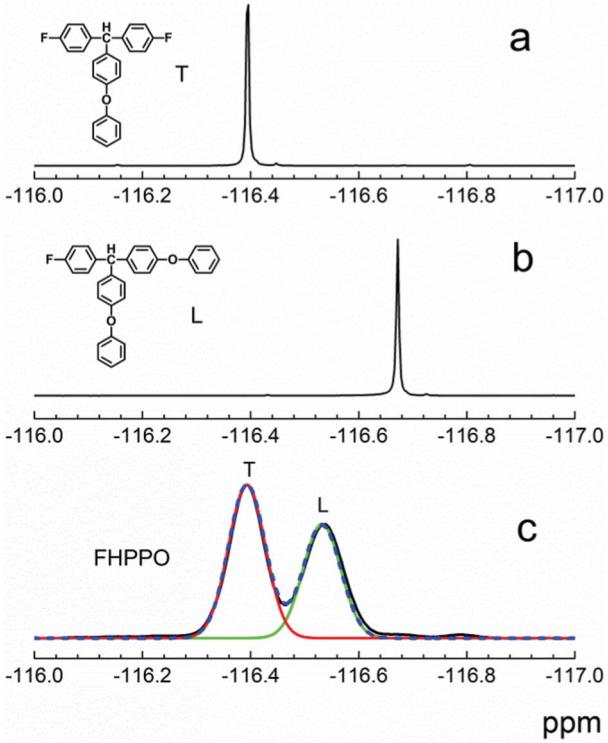

Fig. 5 ^{19}F NMR spectra used to determine the degree of branching of FHPPO: (a) model compound 3, (b) model compound 4. (c) The deconvoluted resonance peaks of observed ^{19}F NMR spectra of FHPPO (solid black line) into terminal (T) and linear (L) structures. The reconstructed spectrum (dotted line) was obtained by summing up the two deconvoluted peaks.

explained by the approximation used in the Holter method, which is more valid for polymers with high molecular weights. We note that the DB values defined by the Holter's method from ^{13}C NMR and ^{19}F NMR are not the same; however, the difference is marginal. Thus, for FHPPO molecules, both ^{13}C NMR and ^{19}F NMR can be used to estimate the DB.

Thermal properties of FHPPO

The DSC curves of FHPPOs with different molecular weights are presented in Fig. 6. All samples show one clear T_g and no endothermic peak was observed below 250 °C. T_g values of FHPPO detected by DSC increase with increasing molecular weight, and the results are summarized in Table 1. The T_g values of FHPPO_1 to FHPPO_5 increase from 135 °C to 164 °C, which are all higher than the T_g of linear PPO ($T_g \approx 95$ °C) with a high molecular weight.[18] The increase in T_g may be ascribed to the highly branched molecular architecture, which can inhibit the mobility of chain segments. It is also noted from Table 1 that the T_g of FHPPOs tends to level off at high molecular weights. This could be explained by the coupled effects of two factors: the portions of the rigid triphenyl structures from the AB_2 monomers, the changes in DB and molecular weights. As molecular weight increases, the proportion of rigid triphenyl groups also increases, which increases the rigidity of the hyperbranched structures and limits the

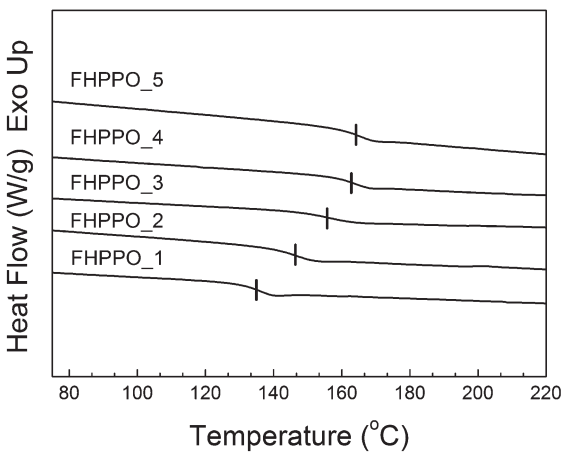

Fig. 6 DSC thermograms of FHPPOs at a heating rate of 10 K min^{-1}.

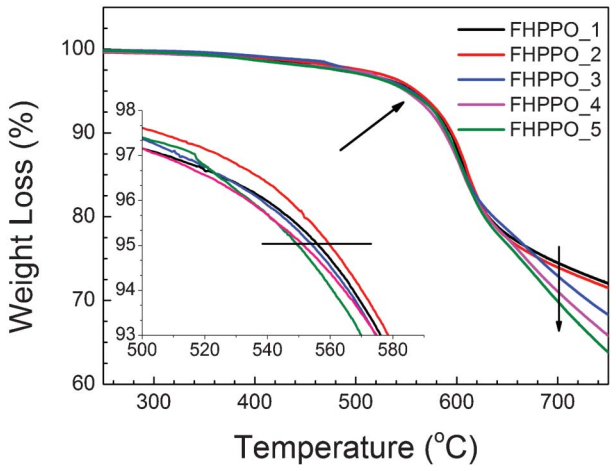

Fig. 7 TGA thermograms of FHPPOs under N_2 atmosphere at a heating rate of 20 K min^{-1}.

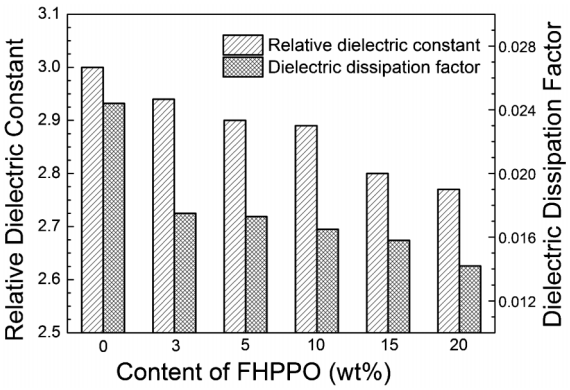

Fig. 8 Dielectric properties of DGEBA/FHPPO composites as a function of FHPPO loading.

mobility of the segments. However, the DB decreases with increasing molecular weight, which means more linear structures in FHPPOs. The increase in linear structures brings in more 'defects' or flexible regions in the hyperbranched structures, resulting in a decrease in the T_g. The change of the T_g with molecular weight is different from that reported in our previous stuides.[32,33]

The weight loss traces of FHPPOs with different molecular weights in nitrogen as a function of temperature are shown in Fig. 7. The values of 5% weight loss temperature (T_{d5}), maximum temperatures of decomposition (T_{max}), and residue at 700 °C are summarized in Table 1. The T_{d5}s of FHPPOs change very little firstly with molecular weight, and then decrease slightly, which cover a range of 549 to 559 °C. The T_{d5}s of FHPPOs are notably higher than those of HPPOs with phenolic terminal groups in our previous study, where the T_{d5}s of the HPPOs were in the range of 258 to 295 °C. This suggests that the terminal groups play an important in the thermal stability of hyperbranched polymers. The T_{max} values of the FHPPOs are all about 600 °C, which are similar to those phenolic-terminated HPPOs.[32] As shown in Fig. 7, the residuals at 700 °C decrease with increasing molecular weight and are above 70%. To sum up, FHPPOs have excellent thermal stability.

Dielectric performance of FHPPO/DGEBA composites

DGEBA/FHPPO composites were prepared by blending different amounts of FHPPO_2 into DGEBA and cured with MNA. Before being cured, the mixtures of FHPPO ($\leqslant$20%) and epoxy/MNA systems were all transparent at room temperature, indicating that homogenous mixtures can be obtained using current mixing procedures. Although FHPPO is a non-reactive modifier for epoxy resins, the hydrogen bonding between fluorine atoms of the FHPPO and hydrogen atoms of epoxy resin can increase the compatibility and lead to homogenous mixtures. DGEBA/FHPPO composites were prepared by curing mixtures following the aforementioned curing procedures. It is expected that the low polarity basic units of PPO, abundant fluoro-terminated groups, and inherent free volumes of FHPPO can improve the dielectric properties of DGEBA/FHPPO composites. The relative dielectric constant (k) and dielectric dissipation factor (D_f) of cured samples at 1 MHz are shown in Fig. 8. Both the k and D_f values of the DGEBA/FHPPO composites are lower than those of the neat epoxy system. The higher the FHPPO content in the composites, the lower the k and D_f values of the FHPPO modified epoxy resins are. At 20 wt% loading of FHPPO, the k value decreased from 3.00 to 2.77, and D_f value decreased from 0.0244 to 0.0142. The decrease of k and D_f in DGEBA/FHPPO can be attributed to the added FHPPO which has lower values of k and D_f. Generally speaking, low-k materials are materials with a dielectric constant of 3.0 or less. When cured with amine, the majority of the unmodified epoxy has a dielectric constant higher than 4.0; when cured with anhydrides, the dielectric constants of the unmodified epoxy generally exceed 3.4. As mentioned above, after addition of the FHPPO, the dielectric constant of the modified epoxy is lowered to 2.77 ($<$3.0). Thus, the FHPPO is a low-k modifier for epoxy resin.

The dielectric properties of epoxy materials depend on lots of factors, including chemical structures, test conditions, and moisture content. As a result, even for the same epoxy resin, different curing agents and test conditions are often used, making the direct comparison between different epoxy systems difficult and misleading. Even so, a comparison is made against some typical low-k modifiers for epoxy materials. Wu[46] used linear polyphenylene oxide (PPO) to modify a DGEBA/cyanate ester curing system. The dielectric constant at 1 MHz decreased from 4.0 of the neat system to 3.5 at 20 wt% PPO loading. In Wang's work,[47] a nanoporous additive, polyhedral oilgomeric silisesquioxane (POSS) which contains eight functional hexafluorine groups (OF), was added into a UV-cured epoxy resin. The dielectric constant decreased from 3.71 of the neat epoxy to 2.80 at 15 wt% OF loading at 100 kHz. In Yung's work,[48] hollow glass microspheres were added into a dicyandiamide-cured epoxy system. The dielectric constant at 1 MHz decreased from 3.98 of the neat system to 3.42 at 20 wt% loading. As mentioned above, the dielectric constant strongly depends on the chemical structure, *i.e.*, the curing agents. In our case, methyl nadic anhydride was chosen for the

curing agent, which leads to a more densely cross-linked, less polar network and more free volume from bicyclic structure than other common curing agents (amine and cyanate ester). Thus, the dielectric constant of the unmodified system is already low (3.0) and further decrease in the dielectric constant is more challenging. At 15 wt% FHPPO loading, the dielectric constant decreased from 3.0 of the unmodified system to 2.8, which has made a quite bit of progress for lower dielectric constant although the improvement is not as big as the examples mentioned above. In addition, the new modifier has good solubility and can form homogeneous solutions upon mixing, which will not complicate the fabrication process. Moreover, after curing, the thermal stability and mechanical properties are improved. (Mechanical and other properties will be reported in more details in future work). Thus, FHPPO is indeed a new promising low-*k* modifier for epoxy.

Free volumes of FHPPO/DGEBA composites

According to the Clausius-Mossotti theory, the dielectric constant can be estimated by the following formula:[49,50]

$$k = \frac{1 + 2(\sum \varphi_i / \sum V_i)}{1 - \sum \varphi_i / \sum V_i} \quad (4)$$

where k is the dielectric constant, φ_i is the molar polarization of each building block, and V_i is the molar volume of each building block. Obviously, decreasing the molar polarization and/or increasing the molar volume of the building blocks can lower the dielectric constant.

Poly(phenyl oxide) (PPO) has a low polarity structure and has been used for electronic materials. C–F bond has low polarizability as well as large molar volume.[43] Therefore, the incorporation of fluorinated substituents into the polymers can effectively lower the dielectric constant by decreasing the molar polarization and by increasing the molar volume. In addition, the hyperbranched polymers contain inherent free volumes or molecule-scale cavities. Thus, the dielectric constant can be further reduced by increasing the molar volume from hyperbranched polymer structures. In addition, the dielectric dissipation factor is proportional to molar polarity. Therefore, the low polarity PPO structure and fluoro-terminal groups in FHPPO can reduce the dissipation factor of the materials. In summary, the lower k and D_f values of DGEBA/FHPPO composites can be related to three factors, *i.e.*, the low polarity structure of PPO backbones, abundant fluoro-terminated groups, which have a large molar free volume and low polarizability of C–F bonds, and the inherent free volume or molecule-scale cavities in the hyperbranched structures. Different from other linear fluorinated polymers, free volume in hyperbranched molecules contributes more to the lowering of dielectric properties, thus a quantitative evaluation of the free volume in the DGEBA/FHPPO composites is very useful.

In order to quantify the free volume in the DGEBA/FHPPO composites, PALS measurements were performed. The results are summarized in Table 3. The lifetime of the *ortho*-positronium (τ_3) corresponds to the size of the individual free volume site, and the intensity (I_3) corresponds to their number concentration. Compared with neat DGEBA, the hyperbranched polymers are found to have more free volume sites both in size and number or concentration (Table 3). The free volume fraction (F_v) can be expressed as

$$F_v = cVI_3 \quad (5)$$

where V is the total volume of a single site of free volume or cavity, which can be calculated from τ_3, c is a constant empirically determined from comparison with pressure-volume-temperature data and is often found to be 0.018 ± 0.002 nm^{-3} for polymers, I_3 is the lifetime of intensity. A detailed background concerning the theory and techniques of PALS can be found elsewhere.[51,52] The results in Table 3 reveal that the free volume fractions of DGEBA/FHPPO composites increase monotonically with increasing FHPPO loading. At 20 wt% loading, the free volume fraction reaches the maximum value of 4.35%, which is *ca.* 27% increase compared with that of the neat DGEBA. The PALS results suggest that the DGEBA/FHPPO composites have more free volume because of the introduction of the FHPPO. The higher free volume of FHPPO comes from two factors: the large molar free volume of fluoro-terminal groups and the molecule-scale cavities from hyperbranched structures.

Moisture resistance of DGEBA/FHPPO composites

The absorbed moisture can act as a plasticizer and impair the mechanical and thermal properties of cured resins. Water has a dielectric constant of 78; thus, even a small quantity of absorbed water in the composites can have adverse effects on the dielectric properties and shorten the service life of low-*k* materials. Therefore, the moisture resistance is also an important parameter for low-*k* materials. As shown in Fig. 9, the moisture absorption (MA) of the DGEBA/FHPPO composites decreases with increasing FHPPO loading. At 20 wt% loading of FHPPO, the MA decreases from 0.539% of the unmodified system to 0.396%. The lower moisture absorption

Table 3 PALS data and free volume fractions of the DGEBA/FHPPO composites

Composition	FHPPO_2 content (wt%)	Lifetime of *ortho*-positronium τ_3 (ns)	Intensity I_3 (%)	Free volume fraction, Fv (%)
Neat DGEBA	0	1.9880 ± 0.0110	19.87 ± 0.41	3.45
3 wt% FHPPO_2	3	1.9372 ± 0.0084	20.57 ± 0.74	3.83
5 wt% FHPPO_2	5	2.0180 ± 0.0100	22.83 ± 0.79	4.11
10 wt% FHPPO_2	10	1.9890 ± 0.0110	23.47 ± 0.65	4.12
15 wt% FHPPO_2	15	1.9610 ± 0.0100	24.70 ± 0.69	4.17
20 wt% FHPPO_2	20	2.0048 ± 0.0092	24.01 ± 0.72	4.35

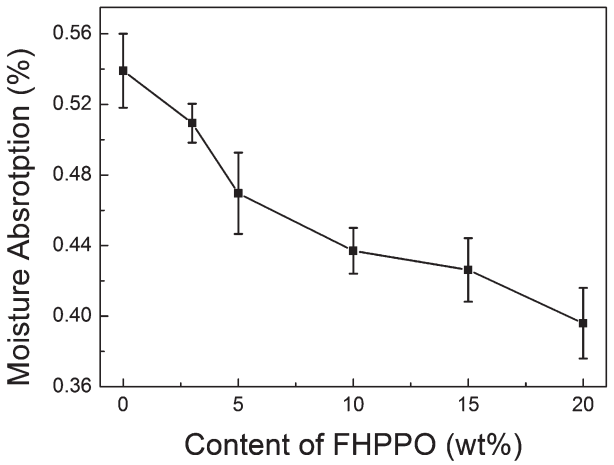

Fig. 9 Moisture absorption of the DGEBA/FHPPO composites as a function of FHPPO loading.

is attributed to the higher content of hydrophobic fluorinated substituents and low-polarity chemical structure of PPO in the skeleton of FHPPO.

The excellent thermal stability, low dielectric constant, low dielectric dissipation factor, and low water absorption make FHPPO a promising additive for epoxy resin in microelectronic applications, such as in semiconductor devices, electromagnetic components, printed circuit boards, and satellite communication equipment.

Conclusions

Using the nucleophilic aromatic substitution (S_NAr) reaction, a fluoro-terminated hyperbranched poly(phenylene oxide) (FHPPO) was readily prepared from a new AB_2 monomer, 4-hydroxyl-4′,4′′-difluorotriphenylmethane. The average molecular weight and the PDI of the FHPPO increased with increasing monomer concentration and reaction time. The chemical structures of the FHPPOs were characterized by ^{13}C NMR and FT-IR, and the degree of branching (DB) of the FHPPOs was estimated by ^{13}C NMR and ^{19}F NMR measurements. The DBs of the FHPPOs decreased with molecular weight. The FHPPOs showed excellent thermal stability and high glass transition temperatures. Because of the low polarity structure of the PPO backbones, abundant fluoro-terminated groups which have large molar free volume, low polarizability of C–F bonds, and the inherent free volume or molecule-scale cavities in the hyperbranched structures, the relative dielectric constant (k), the dielectric dissipation factor (D_f), and moisture absorption of the DGEBA/FHPPO composites apparently decreased after the introduction of FHPPO_2. The increase of free volume with addition of the FHPPO was confirmed by PALS measurements. These excellent dielectric and thermal properties make FHPPO a promising low-k modifier for DGEBA epoxy.

Acknowledgements

This work is financially supported by the National Natural Science Foundation of China (No.2092023, No. 51173012).

Notes and references

1 Y. H. Kim and O. W. Webster, *Macromolecules*, 1992, **25**, 5561–5572.
2 Y. H. Kim and O. W. Webster, *J. Am. Chem. Soc.*, 1990, **112**, 4592–4593.
3 Y. H. Kim, *J. Polym. Sci., Part A: Polym. Chem.*, 1998, **36**, 1685–1698.
4 B. I. Voit and A. Lederer, *Chem. Rev.*, 2009, **109**, 5924–5973.
5 C. Gao and D. Yan, *Prog. Polym. Sci.*, 2004, **29**, 183–275.
6 D. Yan, C. Gao and H. Frey, in *Hyperbranched Polymers: Synthesis, Properties and Applications*, John Wiley& Sons, Inc, New Jersey, 1st edn, 2011, ch.14, pp. 415–440.
7 D. Yan, Y. Zhou and J. Hou, *Science*, 2004, **303**, 65–67.
8 D. Zhang, E. Liang, T. Li, S. Chen, J. Zhang, X. Cheng, J. Zhou and A. Zhang, *RSC Adv.*, 2013, **3**, 3095–3102.
9 Q. Zhu, F. Qiu, B. Zhu and X. Zhu, *RSC Adv.*, 2013, **3**, 2071–2083.
10 D. Wang, H. Chen, Y. Su, F. Qiu, L. Zhu, X. Huan, B. Zhu, D. Yan, F. Guo and X. Zhu, *Polym. Chem.*, 2013, **4**, 85–94.
11 H. Jin, W. Huang, X. Zhu, Y. Zhou and D. Yan, *Chem. Soc. Rev.*, 2012, **41**, 5986–5997.
12 J. Liu, L. Yu, C. Zhong, R. He, W. Yang, H. Wu and Y. Cao, *RSC Adv.*, 2012, **2**, 689–696.
13 M. Zou, J. Fang, J. Liu, C. Li and R. Guan, *Solid State Ionics*, 2012, **220**, 23–31.
14 M. Kakimoto, S. J. Grunzinger and T. Hayakawa, *Polym. J.*, 2010, **42**, 697–705.
15 P. Himmelberg and E. Fossum, *J. Polym. Sci., Part A: Polym. Chem.*, 2005, **43**, 3178–3187.
16 Q. Lin, S. Unal, A. R. Fornof, I. Yilgor and T. E. Long, *Macromol. Chem. Phys.*, 2006, **207**, 576–586.
17 Z. Yu, E. Fossum, D. H. Wang and L. Tan, *Synth. Commun.*, 2008, **38**, 419–427.
18 I. In, H. Lee and S. Y. Kim, *Macromol. Chem. Phys.*, 2003, **204**, 1660–1664.
19 S. Kwak and D. U. Ahn, *Macromolecules*, 2000, **33**, 7557–7563.
20 S. Kwak and H. Y. Lee, *Macromolecules*, 2000, **33**, 5536–5543.
21 C. J. Hawker and F. Chu, *Macromolecules*, 1996, **29**, 4370–4380.
22 H. Satpathi, A. Ghosh, H. Komber, S. Banerjee and B. Voit, *Eur. Polym. J.*, 2011, **47**, 196–207.
23 L. Sennet, E. Fossum and L. Tan, *Polymer*, 2008, **49**, 3731–3736.
24 D. P. Bernal, L. Bedrossian, K. Collins and E. Fossum, *Macromolecules*, 2003, **36**, 333–338.
25 M. Czupik and E. Fossum, *J. Polym. Sci., Part A: Polym. Chem.*, 2003, **41**, 3871–3881.
26 D. P. Bernal, N. Bankey, R. C. Cockayne and E. Fossum, *J. Polym. Sci., Part A: Polym. Chem.*, 2002, **40**, 1456–1467.
27 Y. Seike, Y. Okude, I. Iwakura, I. Chiba, T. Ikeno and T. Yamada, *Macromol. Chem. Phys.*, 2003, **204**, 1876–1881.
28 C. Chiang and F. Chang, *J. Polym. Sci., Part B: Polym. Phys.*, 1998, **36**, 1805–1819.

29 A. Ghosh, S. Chatterjee, S. Banerjee, H. Komber and B. Voit, *J. Macromol. Sci., Part A: Pure Appl. Chem.*, 2011, **48**, 509–517.
30 A. Ghosh, S. Banerjee, H. Komber, A. Lederer, L. Häussler and B. Voit, *Macromolecules*, 2010, **43**, 2846–2854.
31 S. Banerjee, H. Komber, L. Häussler and B. Voit, *Macromol. Chem. Phys.*, 2009, **210**, 1272–1282.
32 J. Zhang, H. Wang and X. Li, *Polymer*, 2006, **47**, 1511–1518.
33 J. Zhang, H. Wang and X. Li, *Chin. J. Polym. Sci.*, 2006, **24**, 413–419.
34 P. Huang, A. Gu, G. Liang and L. Yuan, *J. Appl. Polym. Sci.*, 2012, **123**, 2351–2359.
35 P. Huang, A. Gu, G. Liang and L. Yuan, *J. Appl. Polym. Sci.*, 2011, **120**, 451–457.
36 P. Huang, A. Gu, G. Liang and L. Yuan, *J. Appl. Polym. Sci.*, 2011, **121**, 2113–2122.
37 J. Lv, Y. Meng, L. He, T. Qiu, X. Li and H. Wang, *J. Appl. Polym. Sci.*, 2013, **128**, 907–914.
38 J. Habsuda, G. P. Simon, Y. B. Cheng, D. G. Hewitt, D. R. Diggins, H. Toh and F. Cser, *Polymer*, 2002, **43**, 4627–4638.
39 P. G. Simon, *Trends Polym. Sci.*, 1997, **5**, 394–400.
40 D. M. Bigg, *Polym. Eng. Sci.*, 1996, **36**, 737–743.
41 R. A. Pethrick, *Prog. Polym. Sci.*, 1997, **22**, 1–47.
42 J. Kansy, G. Consolati and C. Dauwe, *Radiat. Phys. Chem.*, 2000, **58**, 427–431.
43 D. W. Van Krevelen and K. T. Nijenhuis, in *Properties of Polymers*, Elsevier, Amsterdam, 4th edn, 2009, ch. 11, pp. 319–354.
44 C. J. Hawker, R. Lee and J. M. J. Fréchet, *J. Am. Chem. Soc.*, 1991, **113**, 4583–4588.
45 D. Hölter, A. Burgath and H. Frey, *Acta Polym.*, 1997, **48**, 30–35.
46 S. J. Wu, T. K. Lin and S. S. Shyu, *J. Appl. Polym. Sci.*, 2000, **75**, 26–34.
47 Y. Wang, W. Chen, C. Yang, C. Lin and F. Chang, *J. Polym. Sci., Part B: Polym. Phys.*, 2007, **45**, 502–510.
48 K. C. Yung, B. L. Zhu, T. M. Yue and C. S. Xie, *J. Appl. Polym. Sci.*, 2010, **116**, 225–527.
49 Y. Kornyushin, *Sci. Sintering*, 2009, **41**, 225–245.
50 O. Ichiro, in *Handbook of Low and High Dielectric Constant Mateirals and Their Applications*, Academic Press, Burlington, 1999, vol. 1, ch 5, pp. 213–240.
51 D. Ratna and G. P. Simon, *J. Appl. Polym. Sci.*, 2010, **117**, 557–564.
52 Y. Y. Wang, H. Nakanishi, Y. C. Jean and T. C. Sandreczki, *J. Polym. Sci., Part B: Polym. Phys.*, 1990, **28**, 1431–1441.

